Effect of Copolymer Addition on Drop Deformation during Uniaxial Elongation and during Relaxation after Cessation of Flow

Nizar Mechbal[†] and Mosto Bousmina*[,†,‡]

Canada Research Chair on Polymer Physics and Nanomaterials, Department of Chemical Engineering (CREPEC), Laval University, Ste-Foy, Québec G1K 7P4, Canada, Hassan II Academy of Science and Technology, Rabat, Morocco

Received June 9, 2006; Revised Manuscript Received December 9, 2006

ABSTRACT: The effect of diblock copolymer addition on the rheological behavior and on the morphology of a PS/PMMA blend during elongation and after cessation of flow is discussed. The blends' morphology was characterized during deformation and at different stages of the relaxation process. Throughout all experiments, the copolymer concentration was selected to fall either below or above the critical concentration of interface saturation. The results show an unexpected fast relaxation at low copolymer concentration, while a much slower stress relaxation is observed at higher concentrations. Such effects were attributed to the competition between hydrodynamic convection of the copolymer molecules and the Marangoni stresses. The local entanglements of the copolymer chains were found to play a major role in such competing effects.

Introduction

Extensional flow is an important component of the complex flow patterns involved in various processes such as extrusion, thermoforming, blow molding, and fiber spinning. In polymer mixtures, extensional flow contributes significantly to the final morphology generated in the molten state as droplets of the minor phase will deform, coalesce, and break, yielding generally a coarse morphology with poor interfacial adhesion between the blend components. To overcome these difficulties, strategies involving either reactive processing or interfacial active agent addition are used. Although some similarities exist between the effects of surfactants and copolymers, we prefer to use throughout this paper the words "copolymer" or "interfacial (or surface) active agent" since their real physics and their structural organization are different.

The presence of the copolymer changes the interfacial properties and therefore it has several effects, among them are the following: (i) it decreases the interfacial tension and therefore it reduces the particles size of the dispersed phase, (ii) it inhibits coalescence and its rate and therefore stabilizes the morphology, (iii) it changes the drop deformation and its mechanism, (iv) it affects the drop breakup in its mode and kinetics, (v) it changes the drop relaxation after cessation of flow, (vi) it reduces and eventually suppresses the interfacial slip while enhancing the wetting and adhesion between the phases, (vii) it alters the phase diagram and the mechanism of phase separation, (viii) it changes heat, mass, and momentum transfer at the interface, (ix) it modifies the interfacial viscosity and elasticity and therefore it changes the interfacial velocity and interfacial stress, (x) it affects the terminal velocity of drops in buoyancy-driven motion, (xi) it damps surface waves in agitated media (known from the Greeks), (xii) it changes the shear-induced particle migration and also the particle migration in thermally nonhomogeneous medium (thermal Marangoni stresses), and (xiii) as a consequence, it affects the final rheological and physical properties of the mixture. Some of these effects have been studied quantitatively, while others were the result of purely qualitative observations. Additionally, only a few studies are available on well-defined systems in well-controlled geometry of flow such as in elongational flow. Here we will focus only on drop deformation and drop relaxation in elongational flow.

For free interfacial agent mixtures of two Newtonian liquids, the droplet deformation is controlled by two dimensionless parameters:[1] (i) the viscosity ratio, p, defined as the ratio between viscosity of the minor phase, η_d, and that of the matrix, η_m:

$$p = \frac{\eta_d}{\eta_m} \tag{1}$$

and (ii) the capillary number, Ca, that expresses the ratio between hydrodynamic stresses, $\eta_m\dot{\epsilon}$, that tend to deform the droplet and eventually to break it and the interfacial stresses, Γ/R, that resist the deformation:

$$\mathrm{Ca} = \frac{\eta_m\dot{\epsilon}}{\Gamma/R} \tag{2}$$

$\dot{\epsilon}$ is the rate of deformation, Γ is the interfacial tension, and R is the initial radius of the droplet. In the case of weak flows (small *Ca*), the droplet is only slightly deformed and adopts an ellipsoidal shape. When such a flow is suppressed, the droplet relaxes and recovers its initial equilibrium spherical shape. If the flow is strong (large Ca), the droplet deforms at high extension; its shape departs from ellipsoidal form and no relaxation to its initial spherical shape is possible when the flow is removed. If the applied flow is very strong (Ca becomes larger than a critical value Ca_{cr}), the droplet deforms at larger extension and adopts a threadlike shape. Such a highly extended shape is not stable, and the droplet will eventually break up to minimize its surface free energy by interfacial tension-driven process. Of course, the shape and the extent of the deformation of the droplet both in the transient and in the steady-state regimes, as well as the mechanism of breakup, change with the viscosity ratio.[2] Such droplet dynamics are now relatively quite well understood at least qualitatively, although the quantitative analytical modeling of the whole process is still missing.

In the presence of an interfacial active agent, the surface tension decreases, and therefore the capillary number increases,

* Corresponding author. E-mail: Bousmina@gch.ulaval.ca. Telephone: 1-418-656-2769. Fax: 1-418-656-5993.

[†] Canada Research Chair on Polymer Physics and Nanomaterials, Department of Chemical Engineering (CREPEC), Laval University.

[‡] Hassan II Academy of Science and Technology.

10.1021/ma061292c CCC: $37.00
Published on Web 01/26/2007

which in turn modifies the droplet deformation. Depending on the extent of deformation, the interfacial agent distribution within the interface may be uniform and can lead to nonuniform deformation. This dual effect of deformation and interfacial agent gradient influences the time evolution of the droplet shape both during the deformation step and during the relaxation occurring after cessation of flow. The effect of flow-induced concentration gradient of insoluble interfacial active agent on drop motion or drop deformation has been studied experimentally by De Bruijn,[3] theoretically by Oldroyd[4] and Flummerfelt,[5] and numerically by Stone and Leal,[6] Milliken et al.,[7] and Milliken and Leal,[8] and by other subsequent works from various authors (Pawar and Stebe,[9] Li and Pozrikidis,[10] etc.). Results have shown that the droplet deformation is not only controlled by the capillary number and the viscosity ratio but also by two additional dimensionless parameters, the surface Péclet number and the interfacial tension ratio. The surface Péclet number is defined as the ratio between the surface convective flux, $\phi_c = \dot{\epsilon}R\Gamma_{eq}$, promoting the concentration gradient and the surface diffusion flux, $\phi_d = D_s\Gamma_{eq}/R$, that tends to restore a homogeneous distribution of the interfacial active agent molecules at the interface:

$$Pe_s = \dot{\epsilon}R^2/D_s \tag{3}$$

where $\dot{\epsilon}$ is the rate of elongation, Γ_{eq} is the interfacial tension at rest, and D_s is the surface diffusivity of the interfacial active agent molecules. The interfacial tension ratio, ψ, is given by:

$$\psi = \Gamma^*(x,t)/\Gamma_0 \tag{4}$$

where Γ_0 is the interfacial tension of the clean interface (without copolymer) and $\Gamma^*(x, t)$ is the local interfacial tension in the presence of the copolymer that varies in space and in time. Note that, for mixtures containing an interfacial active agent, the capillary number has to be rescaled by replacing the interfacial tension by $\Gamma^*(x, t)$. If the four parameters are known, the state of deformation is completely determined for symmetric deformation of an initially spherical droplet.

The modification of the drop deformation arises from the modification of local stresses. In the case of an interfacial active agent modified blend submitted to an axisymmetric flow, the stress jump across the interface is given by:[6]

$$[\mathbf{n}\cdot\mathbf{T}] = -\nabla_s\Gamma + \kappa\Gamma\mathbf{n} \tag{5}$$

where $\mathbf{T}$ is the Cauchy stress tensor, $\mathbf{n}$ is the local unit normal vector, $\kappa = \nabla\cdot\mathbf{n}$ (the divergence of $\boldsymbol{n}$) is the mean curvature of the interface, and ∇_s is the interfacial gradient operator. Equation 5 shows that the stress jump across the interface (represented by the term in the left-hand side of eq 5) is balanced by two effects: the first being the Marangoni stresses ($\nabla_s\Gamma$) that act "tangentially" and arise from the interfacial tension gradient resulting from nonuniform concentration of the interfacial active agent within the interface. The second effect is the Laplace pressure ($\kappa\Gamma\mathbf{n}$) due to the curvature and which acts normally. For high values of Pe_s, it was found that the interfacial active agent molecules are swept toward the tips of the droplet, lowering the local interfacial tension. In such a case, the droplet tips will strongly stretch to increase the local curvature that can balance the pressure jump across the interface (the decrease in Γ should be balanced by an increase in κ to maintain the boundary conditions expressed by eq 4). In contrast, if enough copolymer molecules are swept to the drop tips so that the local concentration approaches the saturation, strong Marangoni stresses are then developed in the opposite direction and the copolymer chains will diffuse from the tips to the equator of the drop to re-establish uniform copolymer concentration. These stresses act tangentially in the opposite direction from the tips to the equator, retarding the convective flux and immobilizing the interface against deformation. At low Pe_s, the interfacial active agent concentration remains almost uniform over the whole interface. Hence, as the interfacial area is increased owing to the distortion of the drop, the interfacial agent concentration decreases and the interfacial tension becomes higher than the initial equilibrium one. Consequently, the drop deformation is reduced.

The influence of surfactant on the deformation and breakup of drops has been investigated numerically by several authors such as Stone and Leal,[6] Milliken et al. ,[7] Milliken and Leal,[8] Pawar and Stebe,[9] Li and Pozrikidis,[10] Eggleton et al.,[11] Blawzdziewicz et al.,[12] Rother et al.,[13] Renardy et al.,[14] Johnson and Borhan,[15] and Yon and Pozrikidis.[16] Experimentally, the effect of compatibilization on drop deformation under shear was studied by many authors. De Bruijn[3] observed that tip-streaming is due to the motion of the interfacial agent from the drop equator to the poles. Such a convective flow increases the drop deformation and changes the mechanism of drop breakup. Levitt and Macosko[17] observed that the presence of a block copolymer increases the deformation as well as the cross-sectional area of the drops. Wang and Velankar[18] carried out strain recovery experiments after cessation of shear and observed that the ultimate recovery after steady shear was increased upon addition of a compatibilizer. They also observed that the compatibilizer slows down the kinetics of the recovery. Van Puyvelde et al.[19] studied the effect of adding low-molecular-weight block copolymer to a dilute mixture of two Newtonian liquids during shear flow. Their results showed that, for blends with small amount of compatibilizer, the drops get highly stretched at the tips. In contrast, for highly compatibilized blends, it was found that the dispersed drops remain almost spherical during shearing.

To our knowledge, no data are available in the open literature on copolymer modified blends during elongation−relaxation flow. The purpose of this work is to examine the effect of diblock copolymer addition on the rheological behavior and the morphology of a model blend made of polystyrene (PS) and polymethyl methacrylate (PMMA) during both elongation and relaxation after cessation of flow. It has been shown in our previous work[20] that the contribution of the components to the total stress of such a blend is very high compared to the interfacial contribution during elongation. For this reason, the focus in the present paper will be mainly made on the relaxation step after the blend has been deformed in uniaxial flow at a given Hencky strain.

Experimental Procedures

Materials and Methods. The uniaxial extensional experiments were carried out using a Rheometric Scientific elongational rheometer RME, which is the commercial version of the elongational rheometer developed by Meissner and Hostettler. To generate uniaxial elongation, the RME uses counter-rotating clamps that grip a rectangular sample from its extremities by means of four belt clamps. The counter-rotating clamps move at constant velocity to stretch the sample exponentially at a constant rate of elongation. The sagging effect is prevented by means of a continuous purge of either air or inert gas at the testing temperature through a porous metal block. More details on this instrument can be found in the paper of Meissner and Hostettler.[21] Because of the high sensitivity of the elongational behavior of polymers, sample preparation and testing were carefully performed as described in our previous work[20] to get accurate and reliable data.

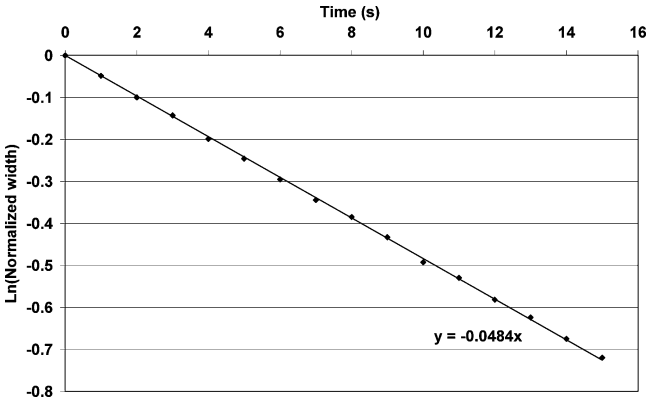

Figure 1. Sample width retraction during elongation at 0.1 s^{-1} and a Hencky strain of 1.5 at 200 °C. The true strain rate was calculated by multiplying the slope of the line fit by −2.

When a flat bar of initial length L_0, thickness B_0, and width W_0 is submitted to uniaxial elongational flow, its dimensions vary exponentially in time according to:

$$L(t) = L_0 \exp(\dot{\epsilon} t) \tag{6a}$$

$$B(t) = B_0 \exp(-\dot{\epsilon} t/2) \tag{6b}$$

$$W(t) = W_0 \exp(-\dot{\epsilon} t/2) \tag{6c}$$

where $\dot{\epsilon}$ denotes the constant rate of elongation imposed on the sample. $L(t)$, $B(t)$, and $W(t)$ denote the evolution of the sample length, thickness, and width, respectively.

The true rate of elongation experienced by the sample should be determined from its deformation history. For this purpose, sample deformation both in length and width was recorded by means of a video camera placed at the top window of the testing chamber of the RME. The natural logarithm of the sample width was plotted versus time, the data were then fitted linearly, and the true elongation rate was obtained by multiplying the slope of the linear fit by −2 owing to:

$$\ln\left(\frac{W(t)}{W_0}\right) = -\frac{\dot{\epsilon}}{2} t \tag{7}$$

For instance, if the set rate of deformation is 0.1 s^{-1}, the true elongational rate obtained by the procedure described above is 0.097 s^{-1} (see Figure 1). Therefore, all of the experiments were carried out without making any correction for the imposed rate of deformation.

Shear flow experiments were performed on the stress-controlled rheometer CVO from Bohlin. The cone and plate geometry (25 mm in diameter) was used for start-up measurements, whereas experiments in oscillatory regime were carried out using a parallel plate geometry (25 mm in diameter) under a continuous purge of nitrogen in order to avoid eventual thermal degradation that may occur during the tests. For both shear and elongational tests, the samples were kept within the cell at the test temperature for 10 min to achieve complete thermal equilibrium before starting the experiments.

The model blend used in this study was made of a commercial polystyrene (PS), supplied by Dow Chemicals, and polymethyl methacrylate (PMMA) from Atohaas America Inc. The interfacial agent used for compatibilization was a diblock copolymer PS-*b*-PMMA purchased from Polymer Source, Inc. Two grades of diblock copolymer were used in order to examine the effect of its molecular weight on drop deformation. The structural characteristics of both homopolymers and diblock copolymers used in this study are shown in Tables 1 and 2, respectively. The molecular weight and molecular weight polydispersity of the homopolymers were measured by gel permeation chromatography (GPC) in THF using linear Waters Ultrastyragel and Shodex KF804 columns equipped with a Waters R401 differential refractometer. Glass-transition temperatures were determined by dynamic scanning calorimetry (DSC) (TA Instruments Q100). The molecular weight and the molecular weight polydispersity of the two diblock copolymers were provided by the supplier.

Table 1. Source, Glass-Transition Temperature, and Molecular Weight of the Homopolymers

polymer (commercial name)	suppliers	molecular weights M_n (g/mol)	molecular weights M_w (g/mol)	T_g (°C)
Polystyrene 685 D	Dow Chemical	122 900	312 400	110
Polymethyl methacrylate	Atohaas America Inc.	50 400	126 600	109

Table 2. Source and Molecular Weight of the Used Copolymers

diblock copolymer	suppliers	M_n (g/mol) PS block	M_n (g/mol) PMMA block	M_w/M_n
PS-*b*-PMMA 1	Polymer Source Inc.	44 000	45 000	1.15
PS-*b*-PMMA 2	Polymer Source Inc.	6500	6500	1.1

Pellets of the pure polymers were initially kept under vacuum at 80 °C for one week. For pure homopolymers and unmodified blends, samples were prepared by melt mixing in a Thermohaake batch mixer at 200 °C at a rotor speed of 45 rpm for 15 min. Disks suited for shear experiments (thickness of 1.2 mm and a diameter of 25 mm) were prepared by compression molding at 200 °C. For elongational tests, the samples were compression molded into rectangular plates of typically 1.5 × 70 × 100 mm^3, from which 10 specimens of size 1.5 × 56 × 7.5 mm^3 were cut by means of a band saw, and their contours were then polished using a Bridgeport milling machine. Compatibilized blends were obtained by adding the copolymer directly in the batch mixer during the melt mixing process. To avoid the alteration of viscoelastic properties of the blends, the amount of block copolymer used in this study was maintained at low values (0.2, 0.5, and 1 wt % with respect to the weight of the dispersed phase). This corresponds to 0.06, 0.15, and 0.3 wt % with respect to the total weight of the blend.

Morphology. Morphological analyses during both elongation and relaxation were obtained by transmission electron microscopy (TEM) using a Jeol JEM 1230 working at 80 kV. Samples intended for morphological analyses were removed from the RME oven at selected stages of elongation and relaxation using a home-made special metal-spring fixture that allows rapid clamping of the stretched samples. Before gripping the samples, the aforementioned metal fixture was immersed into liquid nitrogen for roughly 3 min to accelerate the quenching process. The gripped sample was then further cooled by pouring liquid nitrogen on it during 10−15 s before being cut inside the chamber. The cutoff sample was then quickly taken out of the chamber and immersed again into liquid nitrogen. It was shown in our previous work[20] that for such a blend, this procedure allows quenching of the sample in less than 1 s, which is very small with respect to the drop relaxation time. Consequently, it can be reasonably assumed that the quenching time is short enough to conserve the morphology generated during the imposed deformation and during the relaxation step.

Specimens for TEM were sliced in thin layers using an ultramicrotome. The quenched samples were initially embedded into an epoxy resin (PolyBed 812). Layers of about 8 nm in thickness were cut at room temperature along the flow direction by means of an Ultracut E ultramicrotome from Reichert-Jung equipped with a diamond knife.

Results and Discussion

The dynamic storage and loss moduli, G' and G'', respectively, of the two pure components and of the 30:70 PS/PMMA blends at various levels of compatibilizer (0, 0.2, 0.5, and 1 wt

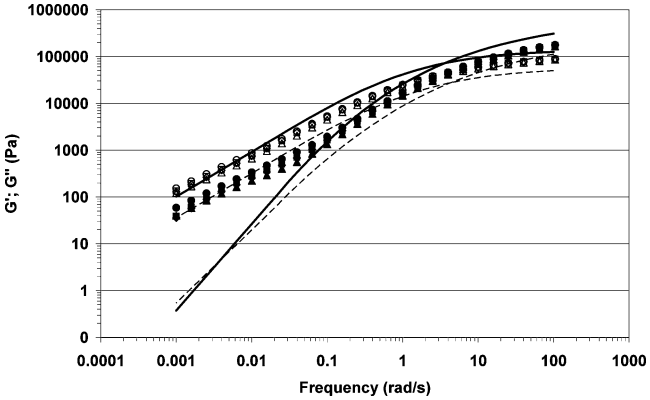

Figure 2. Dynamic shear moduli G' (filled symbols) and G'' (empty symbols) of PMMA (solid line), PS (dashed line), and PS/PMMA 30:70 blend with 0 wt % (▲), 0.2 wt % (■), 0.5 wt % (◆), and 1 wt % (●) of PS-*b*-PMMA 1 diblock copolymer.

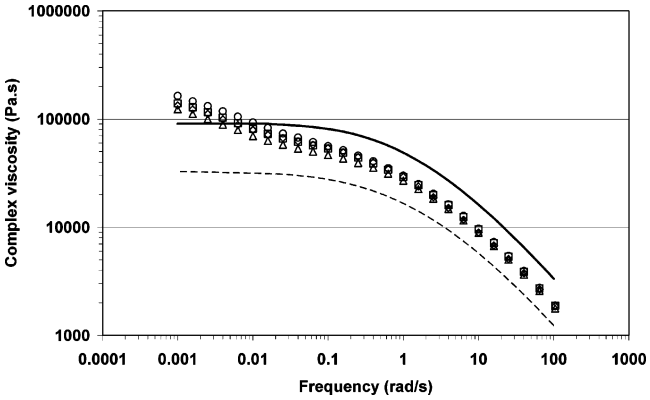

Figure 3. Complex shear viscosity of PMMA (solid line), PS (dashed line), and PS/PMMA 30:70 blend with 0 wt % (▲), 0.2 wt % (■), 0.5 wt % (◆), and 1 wt % (●) of PS-*b*-PMMA 1 diblock copolymer.

%) are shown in Figure 2. Both PS and PMMA exhibit a rubbery plateau at high frequencies and a terminal zone behavior ($G' \approx \omega^2$, $G'' \approx \omega$) at low frequencies, with a terminal relaxation time of 8.14 s for PMMA and 11.25 s for PS. The blends show the classical shoulder on G' in the low-frequency region associated with a slow interfacial relaxation process. The virgin blend is characterized by an additional terminal relaxation time of about 1000 s, which is approximately 100 times the relaxation time of the pure components. The shoulder on G' is more pronounced for the compatibilized blends, with a magnitude that increases with the amount of the compatibilizer. Figure 3 shows that, at low frequencies, the blend components show a Newtonian behavior with a zero shear viscosity of about 90 500 and 32 680 Pa·s for PMMA and PS, respectively. From these values, a low-frequency viscosity ratio of 0.36 is then obtained. At higher frequencies, where the interfacial tension has no role, all blends are characterized by quite the same level of viscosity that lies between the viscosities of the two components. However, at low frequencies and after a short plateau, the blends show again an increase in viscosity that becomes higher than that of the two components. The magnitude of such an increase increases with the wt % of copolymer addition. Addition of a copolymer reduces the interfacial tension and also particle size during the mixing process. Therefore, copolymer-modified blends are characterized by a large interfacial surface area per unit volume that imparts the blend with a large resistance to flow and a large interfacial elasticity.[21,22]

Transient elongational viscosities obtained at an extensional rate of $\dot{\epsilon} = 0.1\ s^{-1}$ for PS, PMMA, and PS/PMMA 30:70 blend

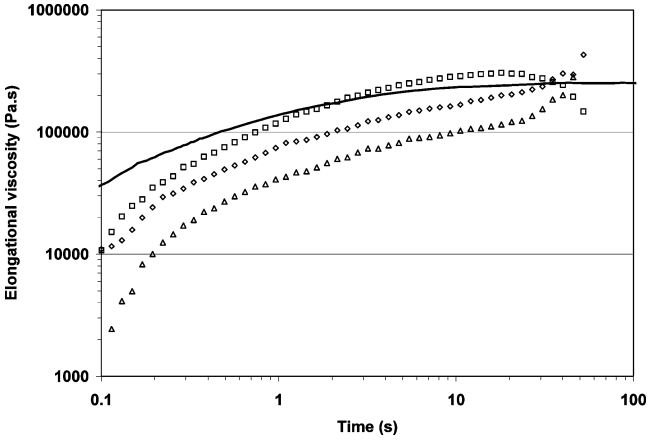

Figure 4. Transient elongational viscosity of PMMA (□), PS (△), and PS/PMMA 30:70 blend (○) at 0.1 s^{-1} and 200 °C. The solid line corresponds to three times the transient zero-shear viscosity of PMMA measured at 0.001 s^{-1} and 200 °C.

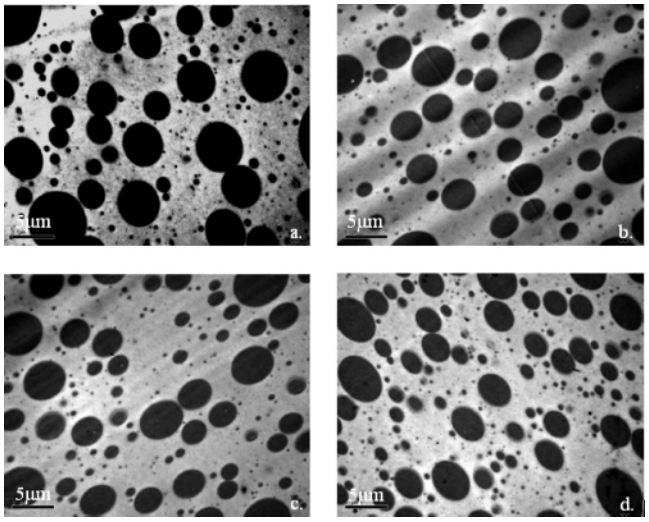

Figure 5. TEM micrographs of PS/PMMA 30:70 blend with (a) 0 wt %, (b) 0.2 wt %, (c) 0.5 wt %, and (d) 1 wt % of PS-*b*-PMMA 1 diblock copolymer.

at 200 °C are plotted in Figure 4. As in shear flow, PMMA shows higher viscosity than PS and the viscosity of the blend lies between the viscosities of PS and PMMA for short times (equivalent to large frequencies in oscillatory shear flow). To compare zero shear viscosity η^0_{shear} and elongational viscosity, an example is shown in Figure 4 for PMMA. Clearly, for a long time in the steady-state regime, the elongational viscosity η_{elong} of PMMA obeys Trouton's law:[23]

$$\lim(t \to \infty)\ \eta_{elong}(t) = 3\eta^0_{shear} \qquad (8)$$

Such a good agreement between elongational and shear viscosities highlights the accuracy of these elongational experiments.

TEM micrographs of compatibilized and uncompatibilized blends before elongation are reported in Figure 5. The blend without a compatibilizer shows spherical PS particles (in dark) with large radii, whereas after compatibilization, a relatively finer morphology is obtained. The slight deformation on the figure is due to the cutting procedure during the sample preparation for TEM observations. The quantitative analysis of the morphology was obtained by means of digital image analyses. The variation of the calculated volume average particle

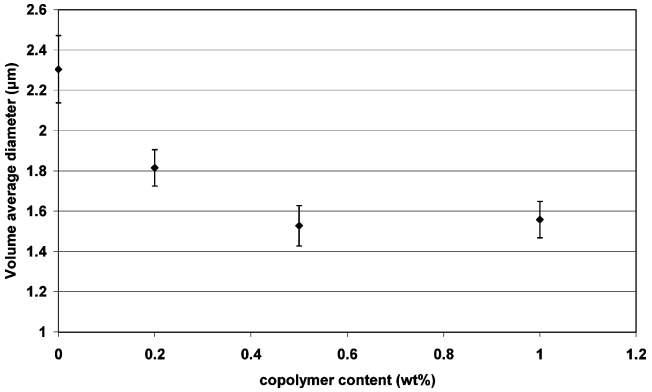

Figure 6. Variation of the volume average diameter of PS drops vs the amount of PS-*b*-PMMA 1 diblock copolymer in the PS/PMMA (30:70) blend.

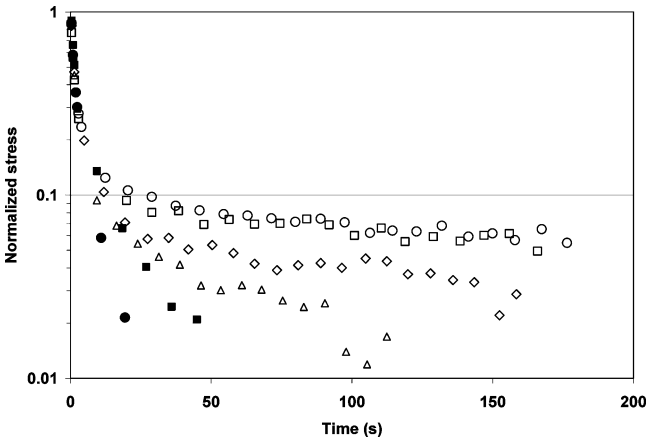

Figure 7. Normalized stress relaxation (stress/last stress reached during the elongation step) after elongation at 0.1 s^{-1} up to 1,5 Hencky strain for PS (●), PMMA(■), unmodified (◇), and copolymer modified PS/PMMA 30:70 blends with 0.2 wt % (△), 0.5 wt % (□), and 1 wt % (○) of PS-*b*-PMMA 1.

radius $\langle R\rangle = \sum N_i R_i^4/\sum N_i R_i^3$ versus the weight percent of the compatibilizer is reported in Figure 6. As can be expected, the average particle size first decreases sharply with the amount of the compatibilizer (C) and then stabilizes when such an amount exceeds a critical value (C_∞). Such a value can be associated with the maximum concentration of the copolymer that can cover entirely the surface of the drops (critical concentration of saturation). To estimate such a critical concentration, we assume that the PS block of the copolymer is completely inside the PS droplets and the PMMA block is located at the interface. The block of PMMA is supposed to be a random coil within an elementary cube located at the surface of the droplet. The center of the random coil of gyration radius R_g coincides with the center of the elementary cube. The complete coverage corresponds to a given number N_c of cubes. The volume of the elementary cube is given by:

$$a^3 = \frac{2\sqrt{2}R_g^3}{3\sqrt{3}} = \frac{R_{ee}^3}{27} \tag{9}$$

where $R_{ee} = R_{ee}^{PMMA}$ is the end-to-end distance of the PMMA block. It is equal to $N^{1/2}b$ (b being the effective bond length) in the case of a linear freely joined chain. The total coverage corresponds to:

$$N_c = 36\pi\langle R\rangle^2/{R_{ee}}^2 \tag{10}$$

The weight fraction of the copolymer at saturation is equal to

$$\mathrm{Wt}_{crit}\,\% = \frac{\rho_{PMMA}N_{PMMA}^S V_{PMMA}^d N_d + \rho_{PS}N_{PS}^S V_{PS}^d N_d}{(4/3)N_d\rho_{PS}\pi\langle R\rangle^3} \tag{11}$$

N_{PMMA}^S and N_{PS}^S are the total number of chains of the blocks PMMA and PS that are present at the interface at saturation, ρ_{PMMA} and ρ_{PS} are their respective densities, and N_d is the number of the drops. Under thermal activation, the random coil of PMMA block fills completely the volume of the elementary cube; therefore, the volume of the elementary cube is equal to the volume of each block of PMMA:

$$V_{block}^d = a^3 \tag{12}$$

The same equation is used for the PS block inside the droplet. Inserting eqs 9, 10, and 12 into eq 11 gives the critical concentration of saturation.

$$\mathrm{wt}_{crit}\,\% = \frac{\rho_{PMMA}R_{ee}^{PMMA} + \rho_{PS}R_{ee}^{PS}}{\rho_{PS}\langle R\rangle} \tag{13}$$

In the present case, the average initial particle size is about 1.6 μm and the end-to-end distance of PS and PMMA are equal to 3.17 and 3.27 nm, respectively. This gives a weight fraction at saturation of about 0.28%. This value is in good agreement with the experimental results reported in Figure 6.

Because of the high viscosity of the blend components, the interfacial contribution to the total stress during elongation is weak relative to the component contribution. Therefore, it is more convenient to examine the relation between the rheological behavior and the evolution of the blends morphology after cessation of the flow during the relaxation step. For each experiment, the sample was stretched at a given rate of elongation up to a given Hencky strain, and then the flow was stopped to measure the stress relaxation. Comparison between the normalized stress relaxation of pure components and of uncompatibilized as well as compatibilized blends after uniaxial elongation at 0.1 s^{-1} up to 1.5 Hencky strain is shown in Figure 7. Here, the stress relaxation was divided by its last value attained during the elongation step, i.e., at $t = 15$ s. As expected, PS relaxes faster than PMMA and the blends take a longer time to relax than their pure components due to the additional interfacial relaxation. The figure also shows that the relaxation stress of the blend compatibilized with 0.5 and 1 wt % of copolymer, particularly in the steady state, is higher than that of the uncompatibilized blend. However, it is curious that the blend with 0.2 wt % of diblock copolymer relaxes faster than the uncompatibilized blend. Experiments were repeated typically three times, and the same behavior was obtained (see, for instance, Figure 8). This behavior seems quite unexpected if one takes into account that adding a block copolymer to an insoluble polymeric mixture tends to reduce the interfacial tension and, consequently, to slow down the stress relaxation. This behavior can be understood in terms of the state of deformation experienced by the drops during the elongational step before the cessation of flow. Such a state of deformation affects the subsequent relaxation process of the drops.

TEM observations were carried out on samples that have been quenched at the end of elongation at 0.1 s^{-1} and at various stages of the relaxation process in order to evaluate the flow-generated morphology as well as its change during the relaxation step after cessation of flow. The obtained typical morphologies are shown in Figure 9 for the uncompatibilized blend and in Figures 10,

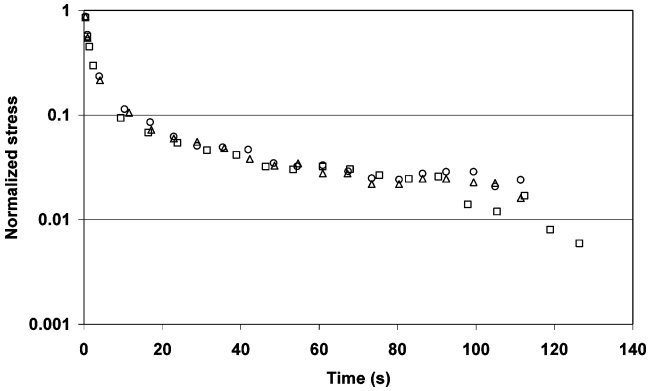

Figure 8. Reproducibility of the normalized stress relaxation for samples with 0.2 wt % of PS-*b*-PMMA 1. The data of the three repeated experiments overlap on the same curve.

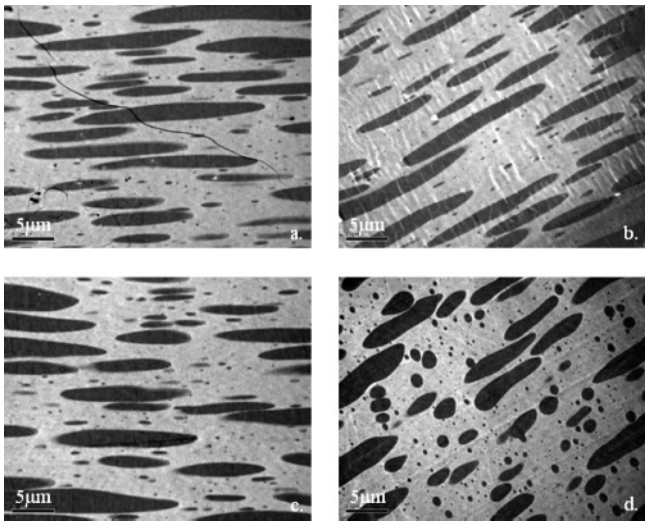

Figure 9. Variation of uncompatibilized PS/PMMA 30:70 blend morphology after elongation at 200 °C and 0.1 s^{-1} (a) up to Hencky strain of 1.5, (b) 40 s, (c) 100 s, and (d) 160 s after the cessation of the flow.

11, and 12 for 0.2, 0.5, and 1 wt % compatibilized blends, respectively. For 0.2 wt % compatibilized blend, the flow-generated morphology is affected by the presence of the diblock copolymer chains at the drop/matrix interface. As evidenced by Figure 10a.2 and a.3, the tips of the PS droplets are clearly stretched. This suggests that a substantial concentration gradient of the copolymer at the interface was generated during the elongation step, leading to a high accumulation of the copolymer molecules at the drop tips. This leads to high deformation as compared to the case of uniform distribution of the copolymer. Hence, copolymer mass transfer is dominated by convection. This can be quantified by the surface Péclet number during the elongation step using eq 3. The surface diffusivity of the copolymer can be estimated from the mutual diffusion coefficient of each block at the vicinity of the interface:[24]

$$D_{AB} = \phi_A \phi_B D_T \left(\frac{1}{N_A \phi_A} + \frac{1}{N_B \phi_B} + 2|\chi| \right) \qquad (14)$$

The Flory−Huggins interaction parameter, χ, is taken here equal to zero because the diffusing components are chemically identical (diffusion of PS in PS and PMMA in PMMA), but

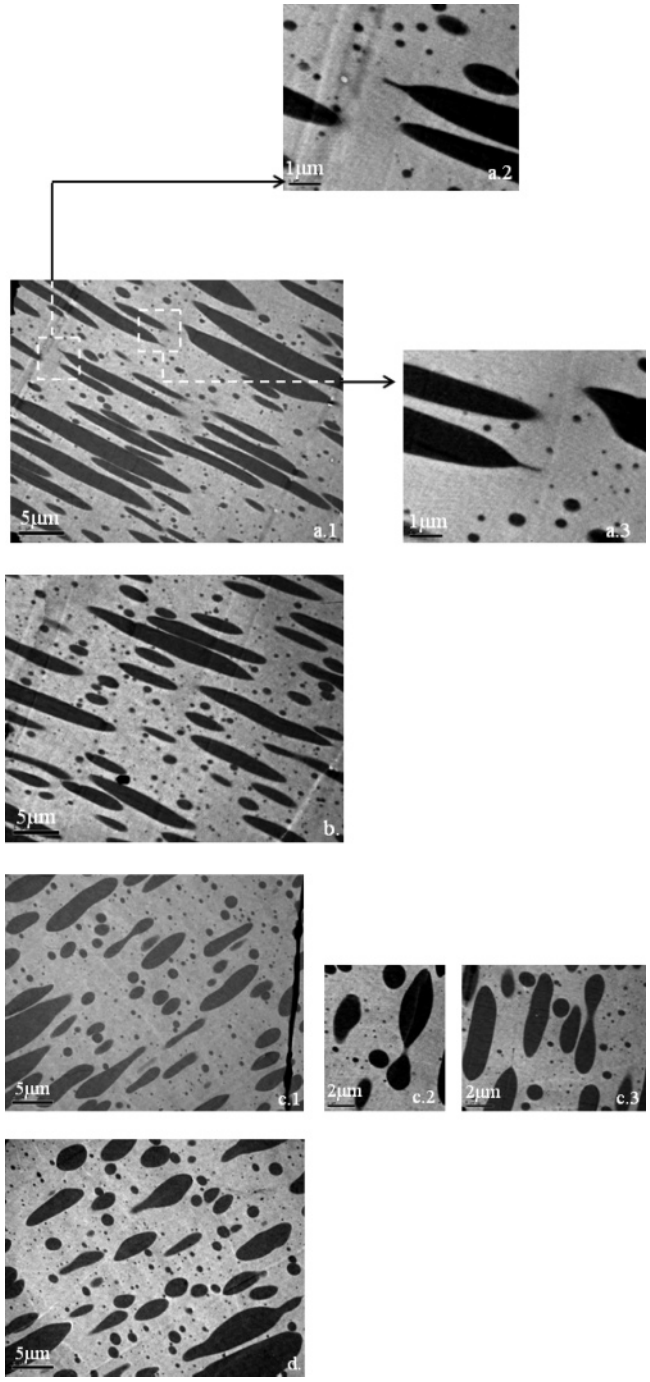

Figure 10. TEM micrographs taken on quenched PS/PMMA 30:70 samples with 0.2 wt % of PS-*b*-PMMA 1 diblock copolymer after elongation at 200 °C and 0.1 s^{-1} (a,1, a,2, a.3) up to Hencky strain of 1.5, (b) 40 s, (c.1, c.2, c3) 80 s, and (d) 100 s after the cessation of the flow.

with different molecular weights. N_i is the degree of polymerization, and D_T is given by fast diffusion model

$$D_T = \phi_A N_B D_B^t + \phi_B N_A D_A^t \qquad (15)$$

where D_i^t is the tracer diffusion coefficient of the component *i* given by:[25]

$$D_i^t = \frac{1}{135} \left(\frac{R_{ee}^i}{M_w^i} \right)^2 \left(\frac{M_e^i \rho RT}{\eta_0^i} \right) \qquad (16)$$

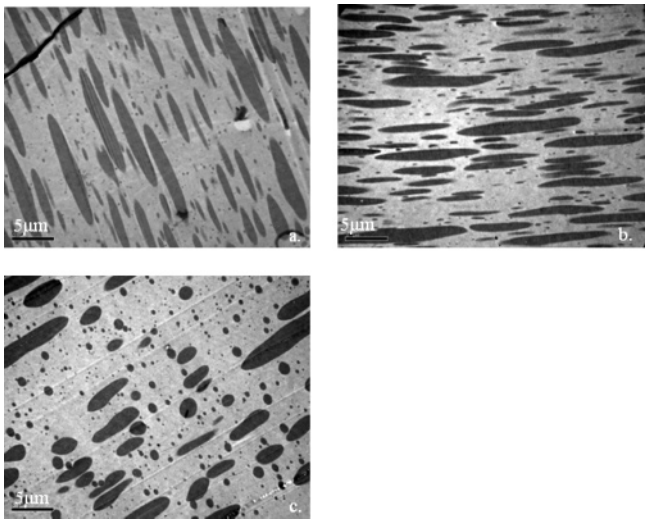

Figure 11. TEM micrographs taken on quenched PS/PMMA 30:70 samples with 0.5 wt % of PS-*b*-PMMA 1 diblock copolymer after elongation at 200 °C and 0.1 s^{-1} (a) up to Hencky strain of 1.5, (b) 40 s, and (c) 200 s after cessation of the flow.

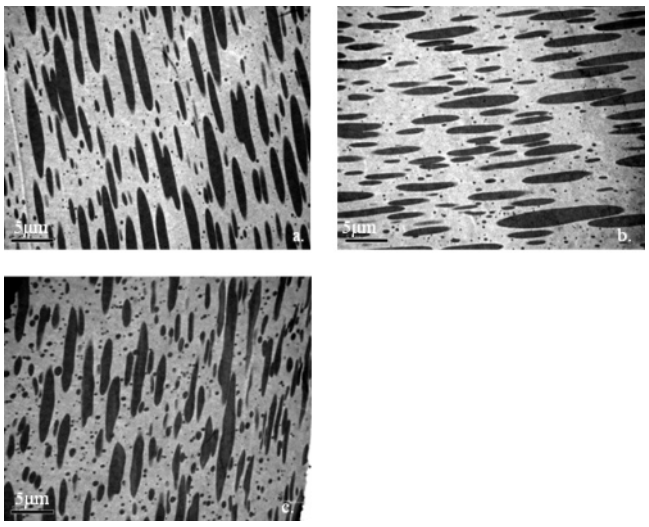

Figure 12. TEM micrographs taken on quenched PS/PMMA 30:70 samples with 1 wt % of PS-*b*-PMMA 1 diblock copolymer after elongation at 200 °C and 0.1 s^{-1} (a) up to Hencky strain of 1.5, (b) 40 s, and (c) 200 s after the cessation of the flow.

where R_{ee} is the end to end distance, M_e the mass between entanglements (9000 for PMMA block and 17 500 for PS block), ρ the density, RT the temperature defined in energy units, M_w^i the molecular weight, and η_0^i the zero-shear viscosity of the component i. The zero-shear viscosity of PS and PMMA blocks is calculated using the following scaling relation:

$$\eta_0 = kM_w^{3.4} \tag{17}$$

To evaluate the fraction ϕ_i, each PS particle is supposed to be surrounded by an outer shell that contains PMMA chains due both to PMMA matrix and PS-*b*-PMMA block copolymer. ϕ_i corresponds then to the ratio of the volume occupied by the PMMA blocks due to the block copolymer over the outer shell volume

$$\phi_{\text{copolymer}} = \frac{(4/3)\langle R\rangle^3 \varphi M_{\text{PMMA/Block}}/M_{\text{copolymer}}}{(4/3)\{(\langle R\rangle + R_{ee}^{\text{PMMA}})^3 - \langle R\rangle^3\}} \tag{18}$$

where φ is the volume fraction of the copolymer. The obtained values for mutual diffusion coefficients for PS and PMMA blocks are 1.3×10^{-13} $cm^2 \cdot s^{-1}$ and 1.45×10^{-15} $cm^2 \cdot s^{-1}$, respectively. The surface diffusivity of the copolymer molecules is then estimated by:

$$\frac{1}{D_s} = \frac{1}{M_{PS} + M_{PMMA}}\left(\frac{M_{PS}}{D_{PS}} + \frac{M_{PMMA}}{D_{PMMA}}\right) \tag{19}$$

This gives a surface diffusivity of about 2.84×10^{-15} $cm^2 \cdot s^{-1}$ and therefore a surface Péclet number of about 590. Such a Péclet number is very high and indicates that, in the case of 0.2 wt % copolymer modified blend, the interfacial dynamics during the elongation step is dominated by the convective flux that promotes the concentration gradient of the copolymer along the drop surface Another way to compare the diffusion and the convection effects during elongation is to calculate the average Marangoni stresses given by:

$$T_{Ma} = \frac{\Gamma^* - \Gamma_0}{\langle R\rangle} \tag{20}$$

where Γ^* is the average interfacial tension in the copolymer modified blend, and the quantity $\Gamma^* - \Gamma_0$ can be estimated by an equation of state such as Van der Waals or Frumkin[26] equations. The later equation is used here with the assumption that interactions among the chains of the copolymer at the interface are weak (local interactions change only slightly the numerical estimation):

$$\Gamma^* - \Gamma_0 = RTC_\infty\left[\ln\left(1 - \frac{C}{C_\infty}\right)\right] \tag{21}$$

where C corresponds to the actual concentration of the copolymer, and C_∞ is its concentration at saturation that was previously calculated by eq 13. The estimation gives an average Marangoni stress of about 40 Pa, which is very small compared to the hydrodynamic stress ($\eta_m\dot{\epsilon}$), which has a magnitude of about 10^4 Pa. Therefore diffusion is negligible with respect to convection.

In the case of high initial surface coverage, i.e., 0.5 and 1 wt % compatibilized blends, TEM micrographs show that PS drops are less deformed than in uncompatibilized and in 0.2 wt % compatibilized blends (see Table 3), which means that, for 0.5 and 1 wt % compatibilized blends, the interface velocity is retarded during the elongation step. This can be attributed to the strong Marangoni stresses that arise in the first stage of elongation as soon as the flow is started. The surface convective flux is then highly counterbalanced, and consequently the interfacial velocity is retarded and the resulting deformation is substantially reduced. From a qualitative viewpoint, these observations can be connected to the critical concentration at saturation (0.28%). In fact, for 0.5 and 1 wt % copolymer addition, the copolymer concentration is above the critical concentration at saturation (0.28%), and therefore the drop surface is entirely covered by PMMA chain blocks that entangle locally. The remaining quantity of the block copolymer will be dispersed in the PMMA matrix in the vicinity of the drops in

Table 3. Values of *L*, *B*, and the Deformation Parameter *D* of PS Drops Having Almost the Same Volume

amount of PS-*b*-PMMA 1 (wt %)	L (μm)	B (μm)	$D = L - B/L + B$
0	7.505	0.722	0.8245
0.2	6.427	0.795	0.7798
0.5	6.262	0.833	0.7652
1	5.901	0.85	0.7481

the form of micelles or alternatively it will form an eventual second diffuse shell (energetically more favorable than micelles formation). As soon as the deformation is started during the elongation step, and if the flow is strong enough to generate disentanglement of the PMMA chains in the adsorbed copolymer layer, the surface of the drop will experience local dilution effects. This generates a gradient of chemical potential that will be immediately restored by diffusion of the block copolymer from the diffuse shell. The situation here is somehow equivalent to mass transfer in blends with a soluble copolymer. The result of such a picture is that the surface deformation is affected by three subsequent or concomitant effects: (i) Marangoni stresses that tend to restore a uniform copolymer concentration over the drop surface, (ii) local entanglements between the PMMA chains of the block copolymer within the adsorbed layer and also with PMMA chains of the matrix, and (iii) the diffuse shell or surface adsorbed micelles act as a reservoir that restores the local uniform concentration of the copolymer at the surface of the drop. Local entanglements render the interface more elastic and slow down the interfacial velocity, which results in a decrease of drop deformation.

Regarding the relaxation step, the TEM micrographs show that the relaxation process of the PS domains in the blend with 0.2 wt % of copolymer is significantly affected by the flow-induced concentration gradient of the copolymer molecules during the elongation step. Some of the deformed drops, especially the largest ones, display considerable strangulation and tend to relax by breaking up into smaller droplets. On the other hand, no break up was found for 0.5 and 1 wt % compatibilized samples. Furthermore, the fast relaxation of the interface in the 0.2 wt % compatibilized blend can be attributed to the concentration profile of the copolymer within the interface at the end of elongation. Indeed, when the flow is stopped, the surface convective flux as well as the surface Péclet number of the droplet falls to zero (see eq 3). Consequently, the copolymer chains will diffuse from the drop tips toward the drop equator in order to restore a homogeneous concentration profile. Significant Marangoni stresses are then developed. These stresses act tangentially and contribute to the fast relaxation of the drops. The Marangoni stresses act here in the relaxation step, whereas for 0.5 and 1 wt %, such stresses act immediately during the first stages of deformation during the elongation step.

The fact that no important tip stretching is observed for 0.5 and 1 wt % of compatibilized blends at the end of elongation suggests that the copolymer chains are more or less homogenously distributed within the interface. The retraction process of PS drops is mainly controlled by the interfacial tension reduction due to the addition of the diblock copolymer rather than by the effect of copolymer chains motion within the interface. As a result, 0.5 and 1 wt % compatibilized blends take more time to relax their stresses than the uncompatibilized blend. A quantitative evaluation of the copolymer concentration profile on the interface of the droplets was attempted by using copolymers containing fluorescent molecules and making local visualization with a confocal microscope. Unfortunately, the obtained pictures were very qualitative and similar to those found by Jeon and Macosko,[27] and therefore, it was not possible to extract from such pictures the copolymer concentration gradient and the resulting Marangoni stresses.

To examine the effect of entanglements of the copolymer chains at the interface, similar experiments were carried out with a diblock PS-*b*-PMMA-2 copolymer having each block characterized by a molecular weight that is smaller than the critical molecular of entanglement of both PS ($M_c \approx 35\,000$ g/mol) and PMMA ($M_c \approx 18\,000$ g/mol). The molecular weights are reported in Table 1. The results of stress relaxation experiments carried out after elongation at 0.1 s^{-1} are reported in Figure 13. The figure shows that adding such a diblock copolymer does not affect the stress relaxation behavior. This confirms that local entanglements evoked earlier are important and influence greatly both the drop deformation during elongation and drop relaxation after cessation of flow.

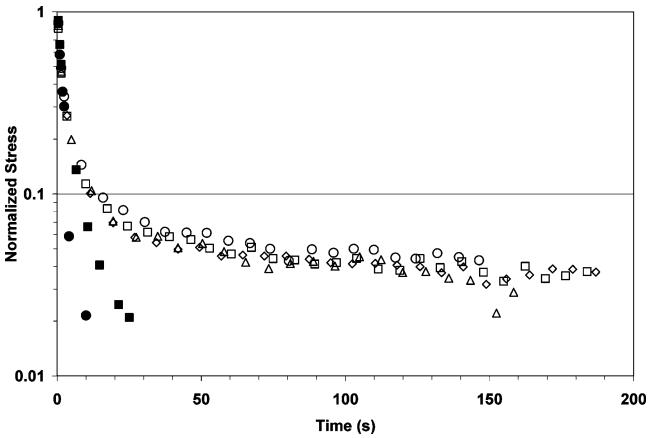

Figure 13. Normalized stress relaxation after elongation at 0.1 s^{-1} up to 1.5 Hencky strain for PS (●), PMMA (■), unmodified (◇), and copolymer modified PS/PMMA 30:70 blends with 0.2 wt % (△), 0.5 wt % (□), and 1 wt % (○) of PS-*b*-PMMA 2 diblock copolymer.

Concluding Remarks

In this work, the effect of diblock copolymer addition on the rheology and on the morphology development was studied experimentally during uniaxial elongation and during relaxation after cessation of flow on PS/PMMA blend with 30% of PS. Concentrations of copolymer (C) both below and above the critical concentration of drop surface saturation (C_∞) were examined. The results showed that, for $C < C_\infty$, the drops are highly extended with tip-streaming effects. Such a behavior was evaluated to be mainly controlled by convection of the copolymer molecules along the interface toward the drop poles. Such a high gradient of copolymer and therefore of interfacial tension generates local Marangoni stresses that act tangentially and accelerate the drop relaxation after cessation of flow. In the case of $C > C_\infty$, the drops are less deformed due to local entanglements that resist the deformation, and therefore, the blend relaxes slowly. When the molecular weight of the copolymer was lower than the critical molecular weight of entanglement for each block, no difference between $C > C_\infty$ and $C < C_\infty$ was observed.

Acknowledgment. This work was financially supported by the NSERC (Natural Sciences and Engineering Research Council of Canada), Canada Research Chair on Polymer Physics and Nanomaterials, and the Steacie Fellowship grants.

References and Notes

(1) Taylor, G. I. *Proc. R. Soc. London, Ser. A* **1932**, *138*, 41−48.
(2) Rallison, J. M. *Annu. Rev. Fluid Mech.* **1984**, *16*, 45−66.
(3) Bruijn de, R. A. *Chem. Eng. Sci.* **1993**, *48*, 277−284.
(4) Oldroyd, J. G. *Proc. R. Soc. London, Ser. A* **1955**, *152*, 567−577.
(5) Flummerfelt, R. W. *J. Colloid Interface Sci.* **1980**, *76*, 330−349.
(6) Stone, H. A.; Leal, L. G. *J. Fluid Mech.* **1990**, *220*, 161−186.
(7) Milliken, W. J.; Stone, H. A.; Leal, L. G. *J. Phys. Fluid A* **1993**, *5*, 69−79.
(8) Milliken, W. J.; Leal, L. G. *J. Colloid Interface Sci.* **1994**, *166*, 275−285.
(9) Pawar, Y.; Stebe, K. *J. Phys. Fluid* **1996**, *8*, 1738−1751.

(10) Lee, J.; Pozrikidis, C. *Comput. Fluids* **2006**, *35*, 43−60.
(11) Eggleton, C. D.; Stebe, K. J. *J. Colloid Interface Sci.* **1998**, *208*, 68−80.
(12) Blawzdziewicz, J.; Vlahovska, P.; Loewenberg, M. *Physica A* **2000**, *276*, 50−85.
(13) Rother, M. A.; Zichenko, A. Z.; Davis, R. H. *Colloids Surf. A* **2006**, *282*−*283*, 50−60.
(14) Renardy, Y. Y.; Renardy, M.; Cristini, V. *Eur. J. Mech. B* **2002**, *21*, 49−59.
(15) Johnson, A. R.; Borhan, A. *J. Colloid Interface Sci.* 199, 218, 184−200.
(16) Yon, S.; Pozrikidis, C. *Comput. Fluids* **1998**, *27*, 879−902.
(17) Levitt, L.; Macosko, C. W. *Macromolecules* **1999**, *32*, 6270−6277.
(18) Wang, J.; Velankar, S. *Rheol. Acta* **2005**, *45*, 741−753.
(19) Van Puyvelde, P.; Velankar, S.; Mewis, J.; Moldenaers, P. *Polym. Eng. Sci.* **2002**, *42*, 1956−1964.
(20) Mechbal, N.; Bousmina, M. *Rheol. Acta.* **2004**, *43*, 119−126.
(21) Doi, M.; Ohta, T. *J. Chem. Phys.* **1991**, *95*, 1242−1248.
(22) Bousmina, M.; Aouina, M.; Chaudhry, B.; Guenette, R.; Bretas, R. E. S. *Rheol. Acta* **2001**, *40*, 538−551.
(23) Trouton, F. *Proc. R. Soc. London, Ser. A* **1906**, *77*, 426−440.
(24) Qiu, H.; Bousmina, M. *Macromolecules* **2000**, *33*, 6588−6594.
(25) Qiu, H.; Bousmina, M. *J. Rheol.* **1999**, *43*, 551−568.
(26) Frumkin, A. Z. *Z. Phys. Chem.* **1925**, *116*, 466.
(27) Jeon, H. K.; Macosko, C. W. *Polymer* **2003**, *44*, 5381−5386.

MA061292C